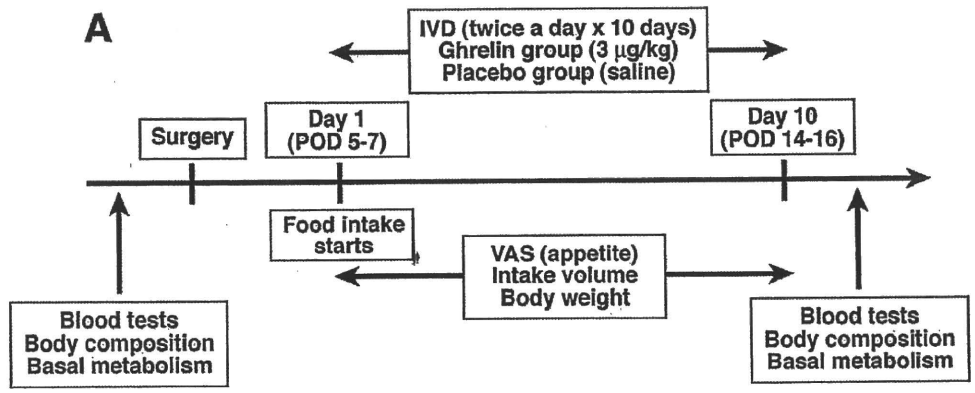

POD; postoperative day, VAS; visual analogue scale; IVD; intravenous drip

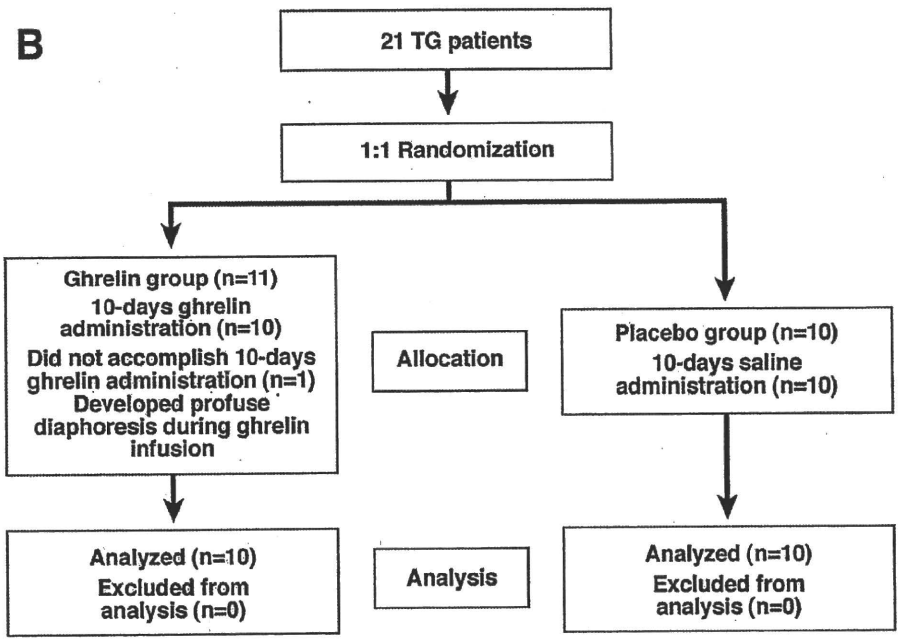

Figure 1. Study protocol and flow diagram.

patient. Body weight was measured with a beam scale to the nearest 0.1 kg, with patients standing barefoot and in light clothing.

Body composition was measured by using dual-energy x-ray absorptiometry (Hologic QDR-2000 instrument; Hologic Inc, Waltham, MA) to assess changes in lean body mass, fat mass, and bone mineral content before and after protocol treatment. The whole body was scanned in the single-beam mode, and the results were analyzed with body composition software. Basal metabolism was measured by using a metabolic analyzer (MedGem metabolic analyzer; HealtheTech, Golden, CO) to assess changes in basal metabolism before and after treatment. All subjects breathed through the MedGem using a disposable, scuba-type mouthpiece. During the measurement, oxygen consumption (VO_2) and body metabolic rate (BMR) were continuously and electronically recorded on a personal computer.

Blood Sampling and Assay

Blood samples were collected from patients before breakfast after an overnight fast, transferred into chilled tubes, stored on ice during collection, centrifuged, serum separated, and stored at −50°C until assay. Insulin-like growth factor (IGF)-I levels were measured by IGF-I IRMA "Daiichi" (TFB, Inc, Tokyo, Japan). Norepinephrine was measured using high-performance liquid chromatography (Tosoh Co, Tokyo, Japan). Cortisol and insulin were measured using the Cortisol Kit "TFB" (TFB, Inc, Tokyo, Japan) and chemiluminescent enzyme immunoassay (Fujirebio, Inc, Tokyo, Japan), respectively. Serum GH and leptin were

measured using GH Kit "Daiichi" (TFB, Inc, Tokyo, Japan) and Human Leptin RIA Kit (Linco Research Inc, St Charles, MO), respectively.

Sample Size Calculation and Statistical Analysis

We estimated that the difference in the effect of ghrelin or placebo on oral food intake calories should be at least 25% assuming 1200 and 1500 kcal/day in the placebo and ghrelin groups, respectively, with ±200 kcal for each SD. To analyze the difference in the effects in the ghrelin and placebo groups using Student *t* test, the study group should comprise at least 16 subjects, with a 5% α value and statistical power of 80%. Assuming that 20% of subjects in each group would not complete the study, the total number of subjects required in this study was estimated at 20.

Numerical values are expressed as mean ± SD unless otherwise indicated. Differences in parameters between the placebo and ghrelin groups were tested by Student *t* test or Mann–Whitney *U* test. Changes in parameters before and after total gastrectomy were tested statistically by the paired *t* test or Wilcoxon signed rank test. Changes in parameters between the 2 groups during the 10 days of follow-up were tested for significance by repeated-measures analysis of variance (ANOVA). A *P* value of <.05 was considered statistically significant. SAS for Windows software version 9 (SAS Institute, Inc, Cary, NC) was used to conduct repeated-measures ANOVA, whereas StatView version 5.0 (SAS Institute, Inc) was used for other tests.

Results

Patient Characteristics

The study flow diagram is summarized in Figure 1*B*. One of the 11 patients (9.1%) in the ghrelin group developed profuse diaphoresis during ghrelin infusion, equivalent to grade 1 by National Cancer Institute Common Terminology Criteria for Adverse Events version 3.0. Accordingly, we decided to stop ghrelin administration and the patient was excluded from further analysis. The 10-day course of ghrelin administration was well tolerated by the remaining 10 patients without any adverse events, although some reported transient periods of feeling warm and/or peristalsis during ghrelin infusion. Table 1 summarizes the clinical background of the 20 patients who completed the study. There was no significant difference in age, sex, body weight, body mass index, and clinical stage of gastric cancer between the 2 groups.

Effects of Ghrelin on Appetite, Food Intake, and Body Weight Loss

Appetite, oral food intake, and body weight were recorded by the patients throughout 10 days of ghrelin/saline administration. During this period, the patients in the 2 groups received the same amount (ie, volume and calories) of intravenous infusion. The mean appetite visual analog scale score was significantly higher in the ghrelin group than the placebo group during the 10-day period (Figure 2*A*; repeated-measures ANOVA, $P = .032$).

Table 1. Patient Characteristics

Parameter	Ghrelin group	Placebo group	*P* value
n	10	10	
Age (*y*)	64.8 ± 10.4	61.6 ± 8.4	.46
Sex (male/female)	7/3	4/6	.19
Body weight (*kg*)	62.2 ± 13.6	62.9 ± 11.5	.89
Body mass index (kg/m^2)	23.1 ± 3.1	24.5 ± 3.8	.36
Procedure (LATG/COTG)	8/2	9/1	.54
Clinical TMN stage			
T (T1/T2/T3/T4)	7/1/2/0	8/2/0/0	.49
N (N0/N1/N2)	9/1/0	9/1/0	1.00
Stage (I/II/III/IV)	8/2/0/0	10/0/0/0	.15

LATG, laparoscopic assisted total gastrectomy; COTG, conventional open total gastrectomy.

Food intake calories (kcal/kg/day) during the 10-day period were significantly higher in the ghrelin group than in the placebo group (Figure 2*B*; repeated-measures ANOVA, $P = .030$). Food intake gradually increased at an earlier period of food intake and was then unchanged thereafter; both groups showed a similar difference throughout the 10-day period. The mean intake calorie over the 10-day period was 13.8 and 10.4 kcal/kg/day for the ghrelin and placebo groups, and ghrelin administration accounted for about 32.7% of the increase.

Body weight loss was calculated in reference to the first day of oral food intake. During this period, body weight gradually decreased in both groups, although the loss was more evident in the placebo group. At the end of the intravenous drip protocol (Day 10), body weight loss was −3.7% for the placebo group but only −1.4% for the ghrelin group. For the 10-day period, body weight loss of the ghrelin group was less than that of the placebo group (Figure 2*C*; repeated-measures ANOVA, $P = .044$).

Effects of Ghrelin on Body Composition and Basal Metabolism

Consistent with the body weight changes, both lean body mass and fat mass decreased gradually during the study period. The mean change in fat mass was −8.8% (14,100 ± 5400 to 12,900 ± 5200 g) and −7.6% (19,000 ± 8400 to 17,700 ± 8300 g) for the ghrelin and placebo groups, respectively. The reduction was statistically significant for each group (Figure 3*A*; $P < .001$). The mean change in lean body mass in the placebo group was −7.8% (41,800 ± 6500 to 38,500 ± 5700 g), which was also significant (Figure 3*B*; $P < .001$); however, the change in the ghrelin group was only −2.9% (44,600 ± 10,500 to 43,200 ± 9600 g, Figure 3*B*; $P = .076$). Figure 3*C* shows the BMR values before and after total gastrectomy. BMR decreased significantly after total gastrectomy in the placebo group (21.8 ± 4.0 to 19.4 ± 3.4

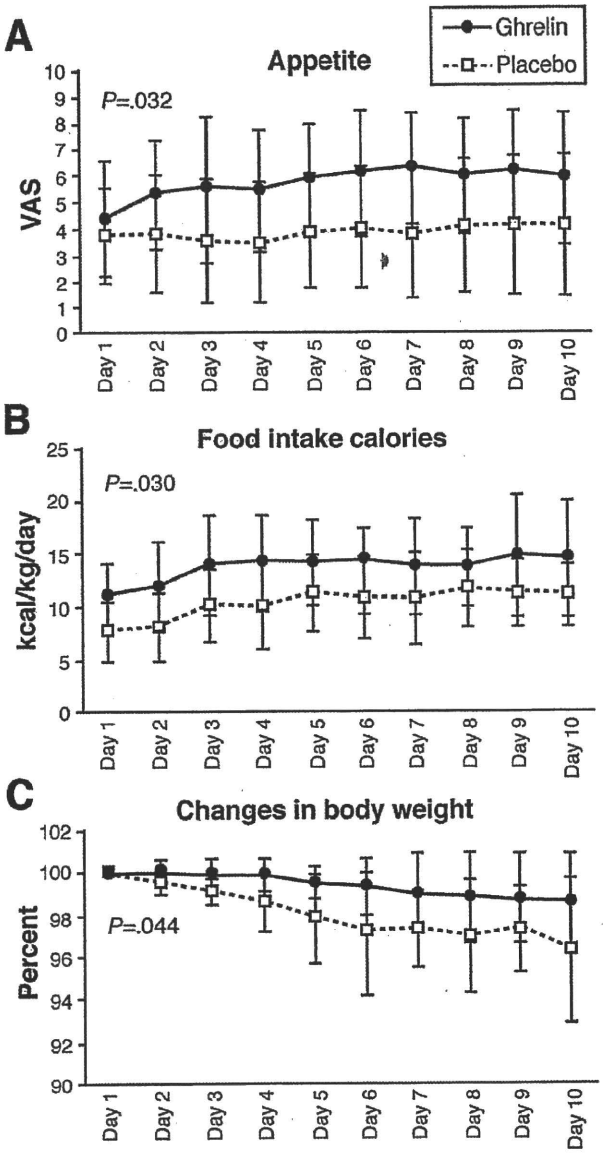

Figure 2. Serial changes in appetite, food intake, and body weight during the 10-day study in the ghrelin and placebo groups. Data are expressed as the mean ± SD of visual analog scale scores of (*A*) preprandial appetite at every meal, (*B*) daily total food intake calories per body weight (kcal/kg/day), and (*C*) percent body weight relative to the first day of oral intake in the ghrelin and placebo groups. The visual analog scale score throughout the study period, which was evaluated by repeated-measures ANOVA, was significantly higher in the ghrelin group than in the placebo group (5.7 vs 3.9 cm; $P = .032$). Likewise, food intake calories were significantly higher in the ghrelin group than in the placebo group (average, 13.8 vs 10.4 kcal/kg/day; repeated-measures ANOVA, $P = .030$). Body weight loss in the ghrelin group was significantly lower than in the placebo group (−1.4% vs −3.7%; repeated-measures ANOVA, $P = .044$).

kcal/kg; $P = .023$). In contrast, the reduction in BMR in the ghrelin group was smaller, and the difference between before and after treatment was not significant (22.6 ± 6.1 to 21.4 ± 6.0 kcal/kg; $P = .20$).

Blood Tests and Hormone Assays

Finally, we compared the results of certain blood tests that reflect the nutritional status and hormones (hemoglobin, total protein, albumin, total cholesterol, triglyceride, leptin, GH, cortisol, norepinephrine, insulin, and IGF-I) both before and after the 10-day period (Table 2). In the early recovery phase, the parameters associated with nutrition did not change in the placebo group but significantly improved in the ghrelin group. Leptin levels decreased significantly in both groups after total gastrectomy, consistent with the reduction in fat mass. On the other hand, there was no significant change in GH, cortisol, norepinephrine, insulin, and IGF-I levels after treatment in both groups.

Discussion

Body weight loss is a common finding in patients who undergo gastrectomy for gastric cancer, which not

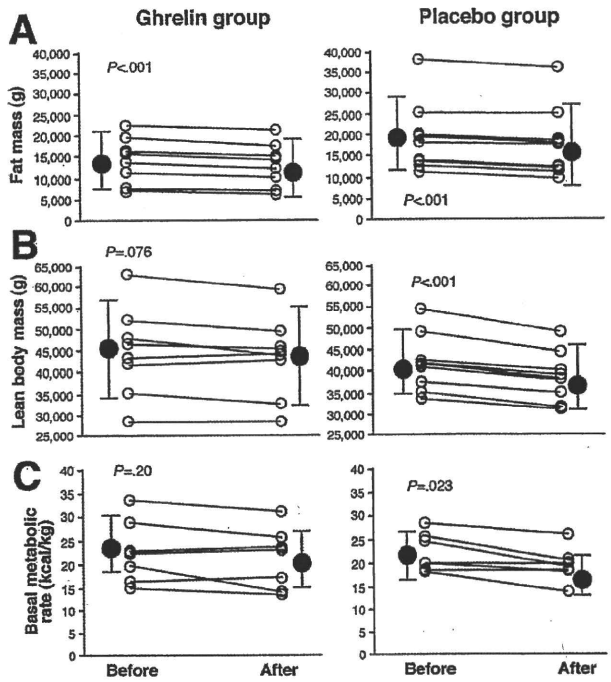

Figure 3. Body composition and basal metabolic rate before and after the study in the ghrelin and placebo groups. (*A*) Fat mass and (*B*) lean body mass measured by dual-energy x-ray absorptiometry and (*C*) basal metabolic rate were determined before and after the 10-day study. Changes for each patient (*open circles*) and the whole group (*closed circles*, ±SD) are shown for the ghrelin and placebo groups. The reductions in all 3 parameters were statistically significant in the placebo group by Student *t* test (fat mass, 19,000 ± 8400 to 17,700 ± 8300 g [$P < .001$]; lean body mass, 41,800 ± 6500 to 38,500 ± 5700 g [$P < .001$]; BMR, 21.4 ± 6.0 to 19.4 ± 3.4 kcal/kg [$P = .023$]). In the ghrelin group, the reduction of fat mass was significant while that of lean body mass and BMR was less than in the placebo group and not statistically significant (fat mass, 14,100 ± 5400 to 12,900 ± 5200 g [$P < .001$]; lean body mass, 44,600 ± 10,500 to 43,200 ± 9600 g [$P = .076$]; BMR, 22.6 ± 6.1 to 21.4 ± 6.0 kcal/kg [$P = .20$]).

Table 2. Results of Laboratory Tests

	Ghrelin group	Placebo group
Hemoglobin (*g/dL*)		
Before	12.2 ± 0.8	12.7 ± 2.4
After	11.8 ± 1.1	11.7 ± 1.4
Total protein (*g/dL*)		
Before	5.7 ± 0.3	6.0 ± 0.7
After	6.6 ± 0.4[a]	6.4 ± 0.3
Albumin (*g/dL*)		
Before	3.1 ± 0.2	3.4 ± 0.6
After	3.5 ± 0.4[a]	3.5 ± 0.2
Total cholesterol (*mg/dL*)		
Before	148 ± 43	176 ± 26
After	174 ± 37[a]	164 ± 32
Triglyceride (*mg/dL*)		
Before	82 ± 47	77 ± 29
After	113 ± 32[a]	99 ± 44
Leptin (*ng/mL*)		
Before	3.1 ± 1.4	7.9 ± 6.7
After	1.2 ± 0.4[b]	4.1 ± 4.0[b]
GH (*ng/mL*)		
Before	0.87 ± 1.5	0.62 ± 0.8
After	0.55 ± 0.7	1.65 ± 2.7
Cortisol (*μg/dL*)		
Before	18.6 ± 4.8	16.9 ± 4.6
After	17.0 ± 4.0	17.9 ± 6.7
Norepinephrine (*pg/mL*)		
Before	314 ± 132	294 ± 171
After	366 ± 122	269 ± 158
Insulin (*μIU/mL*)		
Before	6.1 ± 3.5	10.3 ± 5.5
After	5.1 ± 2.5	6.5 ± 6.0
IGF-I (*ng/mL*)		
Before	108 ± 33	92 ± 36
After	85 ± 53	76 ± 37

[a]$P < .05$, [b]$P < .01$ (paired *t* test; before vs after).

only associates with various pathologic conditions but also affects patients' social activity. Therefore, postoperative body weight loss needs to be investigated thoroughly, especially in Japan, where early gastric cancer accounts for more than 50% of the total incidence of gastric cancer,[30] and the 5-year survival rate of early gastric cancer is more than 90%.[31] Previous studies reported that body weight loss after total gastrectomy was approximately 15% to 20% of the preoperative weight.[10,12,27] Because the incidence of gastric cancer is associated with low body weight in not only Japan and Asian countries but also in the Western world, the estimated average body mass index after total gastrectomy is expected to be 18 to 20 kg/m^2, which is lower than the ideal body mass index. The correlation between low body weight and long-term survival rate has not been analyzed thoroughly even in healthy individuals. A large cohort study of healthy Japanese subjects surveyed over 10 years concluded that a body mass index less than 19 kg/m^2 was associated with high mortality risk at an odds ratio of 2.26 due to various diseases, including infectious, cardiovascular, and malignant diseases.[3] Although there are no concrete data for patients who undergo gastrectomy, these patients could be at risk for a higher mortality rate due to low body weight. Based on this background, the major purpose of this study was to minimize postoperative body weight loss by ghrelin administration through up-regulation of GH secretion and appetite.

At the end of the 10-day study period, ghrelin reduced more than half of postoperative body weight loss from −3.7% in the placebo group to −1.4% in the ghrelin group. Although this is a limited result in the early postoperative period, which is associated with the most profound body weight loss, to the best of our knowledge, ghrelin administration is the most effective procedure among various studies that were designed for the same purpose.[12,32]

After numerous experimental studies, clinical application of ghrelin commenced in healthy volunteers and then extended to patients with heart failure,[23] pulmonary disease,[24] and cancer cachexia.[25] The results of these studies confirmed the safety of ghrelin administration. In our study, the patients in the 2 groups showed no differences in postoperative complications (eg, infections, delayed wound healing, thromboembolism) and length of hospital stay. However, 1 of the 11 patients developed diaphoresis, corresponding to National Cancer Institute Common Terminology Criteria for Adverse Events grade 1. Although we stopped ghrelin administration following the study protocol, this symptom was consistently reported in previous trials although it was tolerated by patients.[23–25,29] The overall positive effects of ghrelin such as body weight gain and increase in food intake calories were observed consistently in all clinical trials, including the present study.[21–25] In addition, improvement of disease-specific status has been reported, including patients with chronic heart failure[23] and those with chronic obstructive pulmonary disease.[24]

To our knowledge, the present study is the first clinical trial in the field of gastroenterological surgery. Moreover, the present study differs in 2 aspects from previous studies.[23–25] The first difference related to the study subjects; the subjects enrolled in previous clinical studies were cachexic emaciated patients in whom the level of circulating ghrelin was predicted to rise. It has been considered that the efficacy of exogenous ghrelin is limited because of down-regulation by high endogenous ghrelin. In contrast, in the present study, in which circulating ghrelin levels were extremely low due to total gastrectomy, we replaced the low levels of endogenous ghrelin with an exogenous one; therefore, it seems more physiologically related to study the effect of ghrelin administration. Another point is that complete vagotomy at the esophagogastric junction was performed during total gastrectomy in our patients. Because the vagus nerve mediates both efferent and afferent ghrelin signals,[33–35] it was suspected that exogenous ghrelin would not adequately interact in the hypothalamus. In animal experiments, vagotomy or chemical blockade of the vagal

signal abolished the effects of intravenously administrated ghrelin.[36] In vagotomized patients, ghrelin administration did not increase food intake.[37] However, other studies reported that ghrelin administered intraperitoneally successfully stimulated food intake after vagotomy in rats[38] and that ghrelin administration in vagotomized patients enhanced GH secretion.[39] These animal experiments and clinical studies indicate that the effects of ghrelin administration are still controversial, at least in vagotomized patients. In the present study, intravenous administration of exogenous ghrelin successfully stimulated food intake and appetite immediately after total gastrectomy. Our results suggest that the administered ghrelin crossed the blood-brain barrier to the central nervous system, probably increasing the appetite signal through not only the vagal pathway but also the circulation. The relationship between ghrelin and vagotomy remains poorly defined, and further studies should be performed in the future.

BMR accounts for between 60% and 70% of the total energy expenditure in adults.[40] Furthermore, the fat-free mass is considered the best single predictor of energy expenditure, and 53% to 88% of the variation in BMR is accounted for by fat-free mass.[41] In the placebo group, the BMR decreased significantly after total gastrectomy, whereas it did not change in the ghrelin group. This result was consistent with the significant decrease in lean body mass, which was limited to the placebo group. In animal experiments, ghrelin enhances abdominal fat storage in white adipose tissue in rats,[19] whereas clinical studies, including the present study, have shown that ghrelin increases lean body mass relative to fat mass.[23,24] Differences in species and patient status may influence the effect of ghrelin administration on fat metabolism. Preservation of lean body mass against the postoperative catabolic metabolism might be caused by ghrelin-stimulated GH secretion from the pituitary gland. However, serum GH levels were stable in the 2 groups, probably due to the rapid turnover of GH. This phenomenon was already reported in a previous phase I study.[29] Baseline leptin levels tended to be lower in the ghrelin group, probably because this group included more men, who generally have lower leptin levels than women.[42,43] Leptin levels significantly decreased in parallel with the decrease in fat mass in both the ghrelin and placebo groups.

The influence of cancer proliferation is another issue of safety in ghrelin studies. Several in vitro studies reported the expression of ghrelin receptor in cancer cells and that ghrelin weakly enhanced their proliferation, for example, in prostate[44] and pancreatic[45] cancer cells. However, another study reported that ghrelin inhibited proliferation and increased apoptosis in a lung cancer cell line.[46] In a preliminary experiment in our laboratory using various gastric cancer cell lines, all cells examined were negative for ghrelin receptor and showed no growth response to exogenous ghrelin (unpublished observation, March 2005). In clinical studies of cancer cachexic patients, no adverse events concerning tumor growth stimulation have been reported.[25] With respect to the present clinical trial, this argument was partly evaded because patients who met the inclusion criteria accounted for more than 90% curability by surgery alone[31] and ghrelin was administered for only 10 days. However, care should be taken when administering ghrelin over longer periods.

Although we successfully demonstrated a short-term effect of ghrelin administration on food intake, appetite, body weight, and other parameters, its long-term effect and benefit still need to be evaluated before clinical application. Because ghrelin secretion does not recover even several years after total gastrectomy, long-term administration of ghrelin is probably required to maintain the short-term effects. For this purpose, ghrelin poses a practical problem in that it is an unstable short-acting peptide and needs to be administered intravenously. An easier administration route, such as subcutaneous injection and inhalation, should be investigated to allow outpatient and home use. GH secretagogues, which were discovered before ghrelin, are orally available and perhaps could be used as ghrelin substitutes. For example, RC-1291 is orally available, well tolerated, and effective in promoting body weight gain, as demonstrated in a phase I study in healthy volunteers.[47] Another issue worth further investigation is the clinical benefits of ghrelin therapy, because it is argued that increases in appetite and body weight are not sufficient reasons for medication. Thus, further studies are needed to evaluate other aspects of ghrelin administration, such as reduction of total medical cost and hospital admission, improvement of social activity and quality of life, and postoperative survival. For example, postoperative body weight loss is most progressive and rehabilitation is most important in the first 3 months after surgery. It is possible that ghrelin administration for at least 3 months would improve postoperative recovery.

In conclusion, this prospective randomized study in a limited number of patients provides convincing data for the beneficial effects of ghrelin on body weight and dietary activity after total gastrectomy. Although there are some issues to be resolved before clinical application, including drug delivery system, duration of administration, and adequate assessment of clinical benefits, surgeons dealing with gastric cancers and other gastroesophageal diseases should be encouraged by the availability of ghrelin. Because surgery is essentially not physiologic and highly invasive for the body but the most reliable therapeutic option to cure cancer, it is our obligation to invent novel procedures to minimize its side effects.

References

1. Demas GE, Drazen DL, Nelson RJ, et al. Reductions in total body fat decrease humoral immunity. Proc Roy Soc B-Biol Sci 2003; 270:905–911.
2. Marinho LA, Rettori O, Vieira-Matos AN, et al. Body weight loss as an indicator of breast cancer recurrence. Acta Oncol 2001;40: 832–837.
3. Tsugane S, Sasaki S, Tsubono Y. Under- and overweight impact on mortality among middle-aged Japanese men and women: a 10-y follow-up of JPHC Study cohort I. Int J Obes Relat Metab Disord 2002:529–537.
4. Bae JM, Park JW, Yang HK, et al. Nutritional status of gastric cancer patients after total gastrectomy. World J Surg 1998;22: 254–260.
5. Friess H, Bohm J, Muller MW, et al. Maldigestion after total gastrectomy is associated with pancreatic insufficiency. Am J Gastroenterol 1996;91:341–347.
6. Melissas J, Kampitakis E, Schoretsanitis G, et al. Does reduction in gastric acid secretion in bariatric surgery increase diet-induced thermogenesis? Obes Surg 2002;12:399–403.
7. Adachi S, Takeda T, Fukao K. Evaluation of esophageal bile reflux after total gastrectomy by gastrointestinal and hepatobiliary dual scintigraphy. Surg Today 1999;29:301–306.
8. Armbrecht U, Lundell L, Stockbruegger RW. Nutrient malassimilation after total gastrectomy and possible intervention. Digestion 1987;37:56–60.
9. Iesato H, Ohya T, Ohwada S, et al. Jejunal pouch interposition with an antiperistaltic conduit as a pyloric ring substitute after standard distal gastrectomy: a comparison with the use of an isoperistaltic conduit. Hepatogastroenterology 2000;47:756–760.
10. Braga M, Zuliani W, Foppa L, et al. Food intake and nutritional status after total gastrectomy: results of a nutritional follow-up. Br J Surg 1998;75:477–480.
11. Bergh C, Sjostedt S, Hellers G, et al. Meal size, satiety and cholecystokinin in gastrectomized humans. Physiol Behav 2003; 78:143–147.
12. Fein M, Fuchs KH, Thalheimer A, et al. Long-term benefits of Roux-en-Y pouch reconstruction after total gastrectomy: a randomized trial. Ann Surg 2008;247:759–765.
13. Liedman B. Symptoms after total gastrectomy on food intake, body composition, bone metabolism, and quality of life in gastric cancer patients: is reconstruction with a reservoir worthwhile? Nutrition 1999;15:677–682.
14. Kojima M, Hosoda H, Date Y, et al. Ghrelin is a growth-hormone-releasing acylated peptide from stomach. Nature 1999;402: 656–660.
15. Date Y, Kojima M, Nakazato M, et al. Ghrelin, a novel growth hormone-releasing acylated peptide, is synthesized in a distinct endocrine cell type in the gastrointestinal tracts of rats and humans. Endocrinology 2000;141:4255–4260.
16. Leite-Moreira AF, Soares JB. Physiological, pathological and potential therapeutic roles of ghrelin. Drug Discov Today 2007;12: 276–288.
17. Shintani M, Ogawa Y, Ebihara K, et al. Ghrelin, an endogenous growth hormone secretagogue, is a novel orexigenic peptide that antagonizes leptin action through the activation of hypothalamic neuropeptide Y/Y1 receptor pathway. Diabetes 2001;50:227–232.
18. Masuda Y, Tanaka T, Inomata N, et al. Ghrelin stimulates gastric acid secretion and motility in rats. Biochem Biophys Res Commun 2000;276:905–908.
19. Davies JS, Kotokorpi P, Eccles SR, et al. Ghrelin induces abdominal obesity via GHS-R-dependent lipid retention. Mol Endocrinol 2009;23:914–924.
20. Wu R, Dong W, Zhou M, et al. Ghrelin attenuates sepsis-induced acute lung injury and mortality in rats. Am J Respir Crit Care Med 2007;176:805–813.
21. Wren AM, Seal LJ, Cohen MA, et al. Ghrelin enhances appetite and increases food intake in human. J Clin Endocrinol Metab 2001;86:5992–5995.
22. Neary NM, Small CJ, Wren AM, et al. Ghrelin increases energy intake in cancer patients with impaired appetite: acute, randomized, placebo-controlled trial. J Clin Endocrinol Metab 2004;89: 2832–2836.
23. Nagaya N, Moriya J, Kangawa K, et al. Effects of ghrelin administration on left ventricular function, exercise capacity, and muscle wasting in patients with chronic heart failure. Circulation 2004;110:3674–3679.
24. Nagaya N, Itoh T, Kangawa K, et al. Treatment of cachexia with ghrelin in patients with COPD. Chest 2005;128:1187–1193.
25. Strasser F, Lutz TA, Maeder MT, et al. Safety, tolerability and pharmacokinetics of intravenous ghrelin for cancer-related anorexia/cachexia: a randomised, placebo-controlled, double-blind, double-crossover study. Br J Cancer 2008;98:300–308.
26. Karamanakos SN, Vagenas K, Kalfarentzos F, et al. Weight loss, appetite suppression, and changes in fasting and postprandial ghrelin and peptide-YY levels after Roux-en-Y gastric bypass and sleeve gastrectomy: a prospective, double blind study. Ann Surg 2008;247:401–407.
27. Takachi K, Doki Y, Ishikawa O, et al. Postoperative ghrelin levels and delayed recovery from body weight loss after distal or total gastrectomy. J Surg Res 2006;130:1–7.
28. Doki Y, Takachi K, Ishikawa O, et al. Ghrelin reduction after esophageal substitution and its correlation to postoperative body weight loss in esophageal cancer patients. Surgery 2006;139: 797–805.
29. Akamizu T, Takaya K, Kangawa K, et al. Pharmacokinetics, safety, and endocrine and appetite effects of ghrelin administration in young healthy subjects. Eur J Endocrinol 2004;150:447–455.
30. Shiraishi N, Yasuda K, Kitano S. Laparoscopic gastrectomy with lymph node dissection for gastric cancer. Gastric Cancer 2006; 9:167–176.
31. Nomura S, Kaminishi M. Surgical treatment of early gastric cancer. Dig Surg 2007;24:96–100.
32. Lehnert T, Buhl K. Techniques of reconstruction after total gastrectomy for cancer. Br J Surg 2004;91:528–539.
33. Asakawa A, Inui A, Kaga T, et al. Ghrelin is an appetite-stimulatory signal from stomach with structural resemblance to motilin. Gastroenterology 2001;120:337–345.
34. Sato N, Kanai S, Takano S, et al. Central administration of ghrelin stimulates pancreatic exocrine secretion via the vagus in conscious rats. Jpn J Physiol 2003;53:443–449.
35. Simonian HP, Kresge KM, Boden GH, et al. Differential effects of sham feeding and meal ingestion on ghrelin and pancreatic polypeptide levels: evidence for vagal efferent stimulation mediating ghrelin release. Neurogastroenterol Motil 2005;17:348–354.
36. Date Y, Murakami N, Nakazato M, et al. The role of the gastric afferent vagal nerve in ghrelin-induced feeding and growth hormone secretion in rats. Gastroenterology 2002;123:1120–1128.
37. le Roux CW, Neary NM, Halsey TJ, et al. Ghrelin does not stimulate food intake in patients with surgical procedures involving vagotomy. J Clin Endocrinol Metab 2005;90:4521–4524.
38. Arnold M, Mura A, Langhans W, et al. Gut vagal afferents are not necessary for the eating-stimulatory effect of intraperitoneally injected ghrelin in the rat. J Neurosci 2006;26:11052–11060.
39. Takeno R, Okimura Y, Iguchi G, et al. Intravenous administration of ghrelin stimulates growth hormone secretion in vagotomized

patients as well as normal subjects. Eur J Endocrinol 2004;151:447–450.
40. Shetty P. Energy requirements of adults. Public Health Nutr 2005;8:994–1009.
41. Nelson KM, Weinsier RL, Long CL, et al. Prediction of resting energy expenditure from fat-free mass and fat mass. Am J Clin Nutr 1992;56:848–856.
42. Kennedy A, Gettys TW, Watson P, et al. The metabolic significance of leptin in humans: gender-based differences in relationship to adiposity, insulin sensitivity, and energy expenditure. J Clin Endocrinol Metab 1997;82:1293–1300.
43. Ostlund RE Jr, Yang JW, Klein S, et al. Relation between plasma leptin concentration and body fat, gender, diet, age, and metabolic covariates. J Clin Endocrinol Metab 1996;81:3909–3913.
44. Yeh AH, Jeffery PL, Duncan RP, et al. Ghrelin and a novel preproghrelin isoform are highly expressed in prostate cancer and ghrelin activates mitogen-activated protein kinase in prostate cancer. Clin Cancer Res 2005;11:8295–8303.
45. Duxbury MS, Waseem T, Ito H, et al. Ghrelin promotes pancreatic adenocarcinoma cellular proliferation and invasiveness. Biochem Biophys Res Commun 2003;309:464–468.
46. Cassoni P, Allia E, Marrocco T, et al. Ghrelin and cortistatin in lung cancer: expression of peptides and related receptors in human primary tumors and in vitro effect on the H345 small cell carcinoma cell line. J Endocrinol Invest 2006;29:781–790.
47. Garcia JM, Polvino WJ. Effect on body weight and safety of RC-1291, a novel, orally available ghrelin mimetic and growth hormone secretagogue: results of a phase I, randomized, placebo-controlled, multiple-dose study in healthy volunteers. Oncologist 2007;12:594–600.

Received July 20, 2009. Accepted December 17, 2009.

Reprint requests

Address requests for reprints to: Shuji Takiguchi, MD, PhD, Department of Gastroenterological Surgery, Osaka University Graduate School of Medicine, 2-2 Suita City Yamadaoka, Osaka, Japan. e-mail: stakiguchi@gesurg.med.osaka-u.ac.jp; fax: (81) 6-6879-3259.

Acknowledgments

Online registry: http://www.umin.ac.jp; clinical trial no. UMIN000001925.

The authors thank Tomoyuki Sugimoto from the Department of Biomedical Statistics, Osaka University, for the advice on statistical analysis as well as the nutritional management room staff of Osaka University Hospital for calculating food intake calories per day in this study.

Conflicts of interest

The authors disclose no conflicts.

Defined factors induce reprogramming of gastrointestinal cancer cells

Norikatsu Miyoshi[a], Hideshi Ishii[a,b,1], Ken-ichi Nagai[a], Hiromitsu Hoshino[a], Koshi Mimori[b], Fumiaki Tanaka[b], Hiroaki Nagano[a], Mitsugu Sekimoto[a], Yuichiro Doki[a], and Masaki Mori[a,b,1]

[a]Department of Gastroenterological Surgery, Osaka University Graduate School of Medicine, Osaka 565-0871, Japan; and [b]Department of Molecular and Cellular Biology, Division of Molecular and Surgical Oncology, Medical Institute of Bioregulation, Kyushu University, Ohita 874-0838, Japan

Communicated by Takashi Sugimura, National Cancer Center, Tokyo, Japan, November 4, 2009 (received for review August 11, 2009)

Although cancer is a disease with genetic and epigenetic origins, the possible effects of reprogramming by defined factors remain to be fully understood. We studied the effects of the induction or inhibition of cancer-related genes and immature status-related genes whose alterations have been reported in gastrointestinal cancer cells. Retroviral-mediated introduction of induced pluripotent stem (iPS) cell genes was necessary for inducing the expression of immature status-related proteins, including Nanog, Ssea4, Tra-1-60, and Tra-1-80 in esophageal, stomach, colorectal, liver, pancreatic, and cholangiocellular cancer cells. Induced cells, but not parental cells, possessed the potential to express morphological patterns of ectoderm, mesoderm, and endoderm, which was supported by epigenetic studies, indicating methylation of DNA strands and the histone H3 protein at lysine 4 in promoter regions of pluripotency-associated genes such as *NANOG*. In in vitro analysis induced cells showed slow proliferation and were sensitized to differentiation-inducing treatment, and in vivo tumorigenesis was reduced in NOD/SCID mice. This study demonstrated that pluripotency was manifested in induced cells, and that the induced pluripotent cancer (iPC) cells were distinct from natural cancer cells with regard to their sensitivity to differentiation-inducing treatment. Retroviral-mediated introduction of iPC cells confers higher sensitivity to chemotherapeutic agents and differentiation-inducing treatment.

cancer stem cells | epigenetics | pluripotent stem cells | embryonic stem cells | differentiation

Cancer is thought to be a genetic and epigenetic disease with uncontrolled proliferative potential. Although the idea was proposed decades ago, the concept that some cancer cells arise from small populations, termed cancer stem cells (CSCs), with both self-renewal potential and multipotential properties sufficient to form tumors, has emerged recently (1, 2). This small population of CSCs possesses persistent self-renewal potential that can be detected by various in vitro assessments and in vivo animal experiments (2). Therefore, it has been proposed that malignant tumors are derived from CSCs with uncontrolled proliferative potential and dysregulation of their mechanisms of differentiation (2).

The origins of CSCs remain incompletely understood (1–3). One view is that CSCs are formed as a result of alterations arising in cells that have already differentiated (1); alternatively, another notion holds that their generation is a result of tumorigenesis that has occurred in immature tissue stem cells or progenitor cells (2); however, in both theories, epigenetic organization participates in tumorigenic regulation (1, 2).

With the investigation and development of ES cells from zygote to blastodermic vesicle stages, the elucidation of the molecular mechanisms that specify pluripotent differentiation has made remarkable progress (4, 5). Regarding the regulation of molecular mechanisms managing this pluripotency, it is obvious that several types of transcription factors specifically discovered in multipotential stem cells display mutual cooperation as a result of epigenetic controls (6–9).

In this study, we analyzed the effects of transcription factor genes that were previously reported in induced pluripotent stem (iPS) cells (6, 7), as well as cancer-related oncogenes and tumor suppressor genes. The repression of tumor-suppressor genes extends the lifespan of embryonic stem (ES) cells or increases the induction efficiency of iPS cells and maintains their immortalized state (10–12). The results indicated that introduction of transcription factor genes into gastrointestinal cancer cells resulted in reprogramming of cells to a pluripotent state and sensitized them to differentiation induction. Such reprogrammed cells were distinct from parental cells. It is hoped that the generation of induced pluripotent cancer (iPC) cells will eventually accomplish some goals in this field. One such goal is the inspection of previously uncharacterized cancer treatments using differentiation therapy via the induction of drug susceptibility in cancer cells. Reprogramming of cancer cells supports the notion that transduction might cause differentiation of cells to unique cell lineages. Another goal is the exploitation of drug discoveries with the aim of producing therapeutic and diagnostic reagents and using them in their clinical applications.

Results

Expression of Genes Inducing Immature Status in Gastrointestinal Cancer Cell Lines. We performed quantitative real-time reverse transcription PCR (RT-PCR) analysis on 20 gastrointestinal cancer cell lines by using immature status-related gene primers for *NANOG, OCT3/4, SOX2, KLF4,* and *LIN28* (Fig. S1*A*). From the results of RT-PCR analysis, we selected cancer cell lines such as DLD-1, HCT116, MIAPaCa-2, and PLC, which exhibited relatively low *NANOG* mRNA expression. In these cells, immature status seems to be effectively exhibited and represented as high *NANOG* expression (6–9). Especially in the colorectal cancer cell line DLD-1, all five selected genes showed relatively low expression compared to the other gastrointestinal cancer cell lines. We then studied the induction of simultaneous combinations of several factors, which include *OCT3/4, SOX2, KLF4,* and *c-MYC*, as well as oncogenes (*BCL2* and *KRAS*) and tumor suppressor genes shRNA (*TP53, P16(INK4A), PTEN, FHIT, RB1*) (Fig. S1 *B* and *C*). These factors were transfected into four cancer cell lines with ecotropic retrovirus produced in PLAT-E packaging cells. Four transcription factors *OCT3/4, SOX2, KLF4,* and *c-MYC* significantly induced up-regulation of *NANOG* mRNA.

Induction of ES-Like State Cancer Cells with Lentiviral and Retroviral Transduction. Induction of human cancer cell lines using lentiviruses and retroviruses requires high transduction efficiencies. We optimized the transduction methods for cancer cell lines (Fig. 1*A*). The four transcription factors, *OCT3/4, SOX2, KLF4,* and *c-MYC*, were transfected into cancer cell lines with ecotropic retrovirus

Author contributions: N.M., H.I., and M.M. designed research; N.M. performed research; N.M. and H.I. contributed new reagents/analytic tools; N.M., H.I., K.N., H.H., K.M., F.T., H.N., M.S., Y.D., and M.M. analyzed data; and N.M. wrote the paper.

The authors declare no conflict of interest.

[1]To whom correspondence may be addressed. E-mail: hishii@gesurg.med.osaka-u.ac.jp or mmori@gesurg.med.osaka-u.ac.jp.

This article contains supporting information online at www.pnas.org/cgi/content/full/0912407107/DCSupplemental.

www.pnas.org/cgi/doi/10.1073/pnas.0912407107

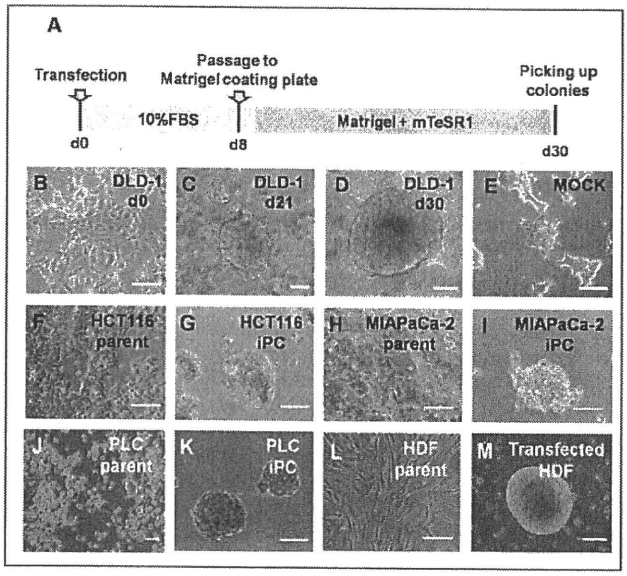

Fig. 1. Induction of human cancer cells with retroviral transduction. (*A*) We optimized the time course of the induction from human cancer cells; the schedule is summarized. (*B–E*) DLD-1 morphology was exhibited. Twenty days later, we observed distinct types of colonies with round shapes (*C* and *D*) that were different from the wild type (*B*). (*E*) Mock was transfected with pMXs Retroviral Vector as a negative control . (*F–K*) Parental and iPC cells of gastrointestinal cancer cell lines from HCT116 (*F* and *G*), MIAPaCa-2 (*H* and *I*), and PLC (*J* and *K*). (*L* and *M*) The referential morphologies are exhibited by HDF. Scale bar: 200 μm. (Original magnification, ×200)

produced in PLAT-E packaging cells. Eight days after transduction, the cells were harvested by trypsinization and plated onto Matrigel-coated plates. The next day, the Dulbecco's modified Eagle medium (DMEM) containing 10% FBS was replaced with the medium suitable for the culture of ES cells. Twenty-one days later, some colonies appeared that were morphologically different from the parental cancer cells (Fig. 1 *B* and *C*). Four weeks after transduction, we observed distinct types of colonies that were different from mock cells, transfected with pMXs retroviral vector as negative control (Fig. 1 *D* and *E*).

We examined the transfection and induction efficiencies by using combinations of *OCT3/4*, *SOX2*, *KLF4*, and *c-MYC*, and compared the results, with four cancer cell lines and human dermal fibroblasts (HDF) serving as controls (Fig. 1 *F–M*). In isolated colonies, we assessed *NANOG* promoter activity, which has been reported to be important in the acquisition of immature status (6–9), by co-transfection of *NANOG* promoter-*GFP* clone. *GFP* expression of transfectants was visualized by fluorescence microscopy (Fig. S2). From 1×10^4 cancer cells, we observed ≈10 *GFP*-expressing sphere formations. These cells in the present study were similar to iPS cells both in morphology, ES-like gene expression and epigenetic modifications as described in refs. 6–9, 13, and 14. Thus, we referred to these cells formed after transduction as iPC cells.

iPC Cells Express ES Cell Markers. Real-time RT-PCR using primers specific for retroviral transcripts confirmed efficient silencing of four retroviruses expressing *OCT3/4*, *SOX2*, *KLF4*, and *c-MYC* in iPC cells (Fig. 2*A*). RT-PCR showed that human iPC cells expressed undifferentiated ES cell-marker genes, including *NANOG*, *OCT3/4*, *SOX2*, *KLF4*, and *c-MYC*, although *NANOG* was not introduced exogenously (Fig. 2*B*). iPC cells expressed ES cell-specific surface antigens (15) including Ssea-4, tumor-related antigen (Tra)-1-60, Tra-1-81, and Tra-2-49 (Fig. 2 *C–G*) compared to the negative control (Fig. 2*H*).

In Vitro Differentiation of iPC Cells. To determine the differentiation ability of iPC cells, we used floating cultivation as embryoid bodies (EBs). Because iPC cells formed ball-shaped structures in suspension culture, we transferred these EB-like structures to EB culture conditions (EBC). These conditions were gelatin-coated plates maintained in DMEM/F12 containing 20% knockout-certified serum replacement. Culture was continued for another 7 days (Fig. 3*A*). Attached cells, named PostiPC cells, began to proliferate after 48 h. PostiPC cells were analyzed by the experiments described below and were compared to parental and iPC cells.

To determine the differentiation ability of iPC cells in vitro, we introduced iPC cells according to the methods of iPS (7). PostiPC cells showed various types of morphology, resembling those of epithelial cells, mesenchymal cells, and neuronal cells (Fig. 3 *B–E*). Immunocytochemistry detected cells that were positive for keratin 19 (Krt19) representing endoderm, vimentin (Vim) representing mesoderm and parietal endoderm, bIII-tubulin (Tubb3) representing ectoderm, and glial fibrillary acidic protein (Gfap) representing ectoderm (Fig. 3 *F–I*). RT-PCR confirmed, in addition to *VIM*, the expression of *FABP4* representing mesoderm, microtubule-associated protein 2 (*MAP2*) representing ectoderm, and paired box 6 (*PAX6*) representing ectoderm in PostiPC cells (Fig. 3*J*). The expression of *CDH1* representing endoderm and *KRT19* decreased in PostiPC cells. In particular, the gene expression of mesoderm and endoderm was increased in PostiPC cells, which was low or difficult to detect in the parental cells.

We then examined whether lineage-directed differentiation of iPC cells could be induced by methods reported for mesenchymal stem cells. We seeded iPC cells with supplements

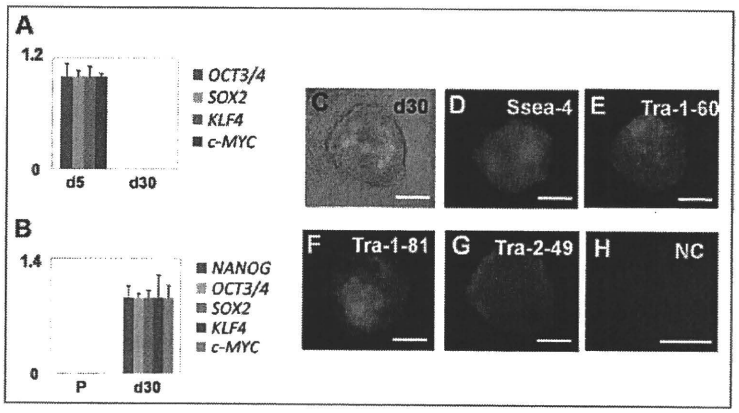

Fig. 2. iPC cells induced from DLD-1 expressing ES cell markers. (*A*) Real-time RT-PCR using primers specific for retroviral transcripts confirmed efficient silencing of four retroviruses expressing *OCT3/4*, *SOX2*, *KLF4*, and *c-MYC*. The mean value of d5 was set to 1 in each transcript. (*B*) iPC cells expressed undifferentiated ES cell-marker genes, including *NANOG*, *OCT3/4*, *SOX2*, *KLF4*, and *c-MYC*. The mean value of d30 was set to 1 in each transcript. (*C–G*) iPC cells were analyzed for several surface antigens, phase contrast (*C*), Ssea-4 (*D*), Tra-1-60 (*E*), Tra-1-81 (*F*), Tra-2-49 (*G*) and negative control (H). P, parental cells; NC, negative control. Scale bar: 200 μm. (Original magnification, ×200)

CELL BIOLOGY

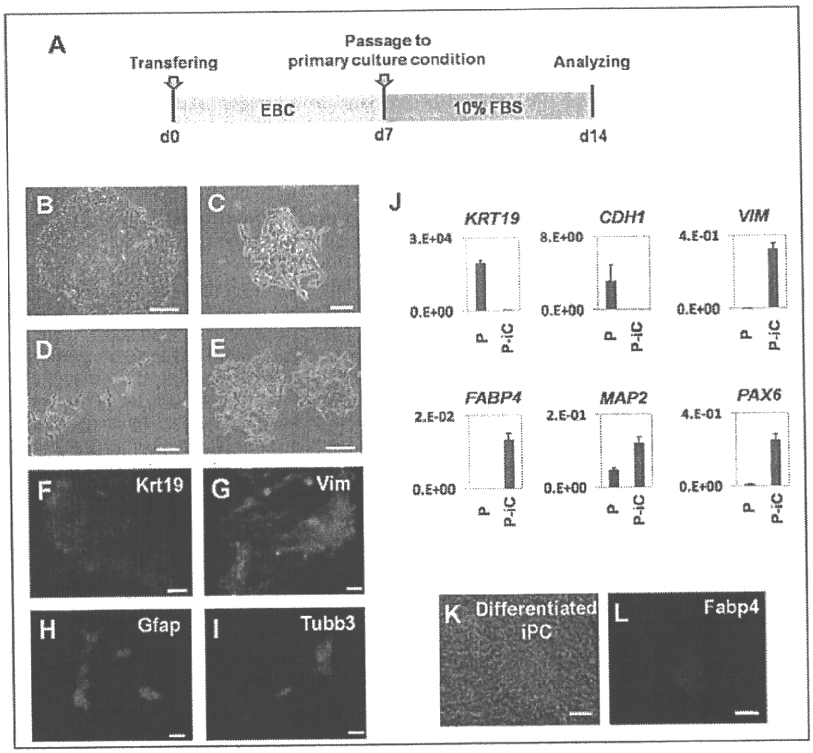

Fig. 3. Embryoid body (EB)-like formation mediated differentiation of iPC cells induced from DLD-1. (*A*) Schedule of induction from iPC cells to PostiPC cells. (*B–E*) After forming EB-like structures, iPC cells were transferred to primary culture conditions. Seven days later, attached (PostiPC) cells showed various morphologies, resembling those of epithelial cells (*B*), mesenchymal cells (*C*), neuronal cells (*D*), and mixed (*E*). (*F–I*) Immunocytochemistry confirmed the expression of Krt19 (*F*), Vim (*G*), Gfap (*H*), and Tubb3 (*I*) in these cells. (*J*) Real-time RT-PCR analysis verified the expression of differentiation markers, such as *KRT19, CDH1, VIM, FABP4, MAP2,* and *PAX6*. The expression of mRNA copies was normalized against *GAPDH* mRNA expression. (*K* and *L*) Directed differentiation of iPC cells into adipocytes showed differentiated iPC cells (*K*) that were positive for Fabp4 (*L*). P, parental cells; P-iC, PostiPC cells.

inducing adipocytes and maintained them under differentiation conditions for 2 weeks. The cells proliferated and immunocytochemistry detected cells positive for Fabp4 (Fig. 3 *K* and *L*). In contrast, immunocytochemistry on parental cells in the corresponding culture detected cells that were negative for Fabp4. These data demonstrated the possibility that iPC cells, compared to parental cells, could differentiate into three germ layers in vitro and indicated that cells acquired different properties.

Epigenetic Modification of Immature Status-Related Genes. Bisulfite genomic sequencing analyses were used to evaluate the methylation statuses of cytosine guanine dinucleotides (CpG) in the promoter regions of pluripotent-associated genes such as *NANOG*. The results revealed that the CpG dinucleotides of *NANOG* promoter were less methylated in transfected HDF (T-HDF) cells and two iPC clones, whereas the nucleotides were methylated in HDF, parental cancer cells, and PostiPC cells (Fig. 4*A*). Chromatin immunoprecipitation with trimethyl-histone H3 protein at lysine 4 (H3K4) antibody was used to analyze histone modification (Fig. 4*B*). The histone modification analyses for *NANOG* gene promoter showed that H3K4 was trimethylated in iPC, PostiPC, and T-HDF (14), whereas that of parental cancer cells and HDF was not detected. Similarly, the H3K4 trimethylation of *OCT3/4* gene promoter increased in iPC, PostiPC, and T-HDF, compared to parental cancer cells and HDF, respectively. The trimethylation of *SOX2* gene promoter was detected before and after the reprogramming of cancer cells, whereas the trimethylation of T-HDF, but not HDF, was detected. The trimethylation of *PAX6* and *MSX2* gene promoter was not detected. These findings demonstrated activation of the promoter regions of immature status-related genes in iPC cells.

Gene Expression and iPC and PostiPC Surface Markers. PostiPC cells, but not iPC cells, showed increased expression of several differentiation markers such as *FABP4, MAP2,* and *PAX6* (Fig. 3*J*), and markedly decreased expression of *NANOG*, *REX1*, *OCT3/4*, *SOX2*, *KLF4,* and *c-MYC*, which corresponded to those of parental cells (Fig. 5*A*). The expression of *P16(INK4A)* in PostiPC cells increased more than that in parental cells.

In colorectal cancer, the surface markers for CD24 and CD44 have been reported as CSC markers (16, 17). Flow cytometry showed that CD44 expression was markedly reduced in iPC cells and was increased in PostiPC cells. The CD44 expression level was relatively low in PostiPC cells compared with that of parental cells (Fig. 5*B*). CD 24 expression level was not changed apparently. The results showed the transition of the population from parental cells to PostiPC, suggesting an alteration of biological characteristics, such as sensitivity to chemicals.

Sensitivity of Anticancer Drug and Differentiation-Inducing Chemicals. The methyl thiazolyl tetrazolium (MTT) assay showed that PostiPC cells acquired sensitivity to 5-fluorodeoxyuridine (5-FU) to a greater degree than parental cells ($n = 11$, $P = 0.003$, Wilcoxon rank test; Fig. 6*A*). These data suggest the possibility that PostiPC cells, via iPC cells, could be more sensitive to therapeutic agents.

Proliferation assays for 48 h in Matrigel and the mTeSR1 medium, an ES-culture condition, showed that iPC cell growth significantly decreased compared with parental cells based on mean cell counts in four independent wells ($n = 4$, $P = 0.046$, Wilcoxon rank test; Fig. 6*B*). There was, however, no significant difference in 48-h proliferation of parental and PostiPC cells in primary culture conditions (Fig. 6*C*). An invasion assay showed no significant differences between parental and PostiPC cells (Fig. 6*D*). In a sharp contrast, the 48-h proliferation assays with the presence of retinoic acid (RA) and 1,25-dihydroxy vitamin D3 (VD3), which are known as inducers of differentiation (18, 19), resulted in a reduction in PostiPC cells compared with mock-treated parental cells ($n = 8$, $P = 0.512$ and 0.049, respectively, Wilcoxon rank test; Fig. 6 *E* and *F*). Invasion assays were performed after the 48-h treatment; the data indicated that, in the presence of RA and VD3, the invasion activity of PostiPC cells was reduced compared with parental cells ($n = 6$, $P = 0.013$ and 0.003, respectively, Wilcoxon rank test; Fig. 6 *G* and *H*).

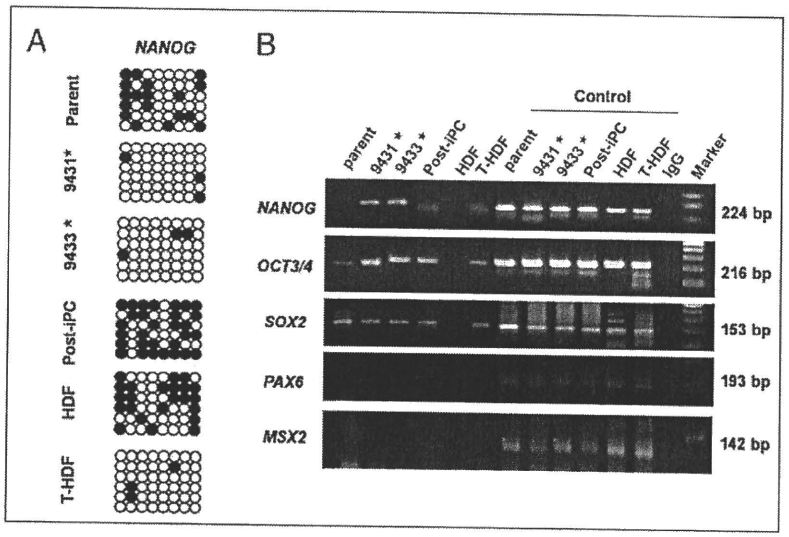

Fig. 4. Epigenetic modification of immature status-related genes evaluated with bisulfite sequencing analysis and chromatin immunoprecipitation in DLD-1. (*A*) From the analysis of epigenetic status, bisulfite genomic sequencing analyses in the promoter regions of genes inducing immature status, *NANOG*, revealed that they were not methylated appreciably in iPC cells (clones 9431 and 9433), whereas the CpG dinucleotides of the regions were methylated in parental cancer cells and PostiPC cells (open and closed circles indicate unmethylated and methylated, respectively). (*B*) Chromatin immunoprecipitation with trimethyl-K4 H3 antibody was used to analyze the histone modification status in parental, iPC, and PostiPC cells. H3 lysine 4 was methylated in these regions for *NANOG* in iPC cells compared to that in parental and PostiPC cells. H3 lysine 4 was methylated in these regions for *OCT3/4* in iPC and PostiPC cells compared to those in parental cells (results were assessed in contrast to each input DNA). HDF and transfected HDF (T-HDF) were analyzed for comparison. As a control, respective sheared chromatin sample was used for quantitative PCR. *, clones of iPC cells.

Assessment of Tumorigenic Properties. To determine tumorigenic properties in vivo, PostiPC cells were transplanted s.c. at several densities into dorsal flanks of NOD/SCID mice. Four weeks after injection, we observed tumor formation (Fig. S3*A*). There were significant differences between PostiPC cells and parental cells ($P < 0.01$, Wilcoxon rank test; Fig. S3*B*). These data demonstrated the reduction of tumorigenesis via reprogramming process; this finding may be applied to anticancer therapy.

Discussion

The role of CSCs was noted in acute myeloid leukemia (3). The possible involvement of CSCs has since been shown in several solid tumors (20–22). In solid tumors, these results suggest that the CSC population, although it is likely a minority, is related to treatment resistance and problems of relapse or metastasis (1, 2). CSCs, through their self-renewal and drug-resistant capacities, may share properties that are conducive to persistence and proliferation, even after anticancer therapy. It is important to understand their biological characteristics, as specific markers of all CSCs have not yet been identified.

Recently, several reports have shown that tumor development is associated with genetic and epigenetic changes of the genome, and that epigenetic modifications play an important role in tumor heterogeneity (23). Several experiments, such as nuclear transplantation, ES cell fusion, and transfection with several transcription factors, have demonstrated reprogramming of terminally differentiated cells into pluripotent embryonic cells, which is linked to the development of an organism by resetting the epigenetic modifications (4–9). In previous reports, the transcription factor *NANOG* was required to maintain the pluripotency and self-renewal of ES cells (13, 14).

According to genetic and epigenetic analyses in previous reports, immature status related to promoter activation in defined genes, such as *NANOG*, plays a very important role in the establishment of a pluripotent state (6–9, 13, 14). To prepare iPC cells, we manufactured a specific tool that could detect the pluripotent

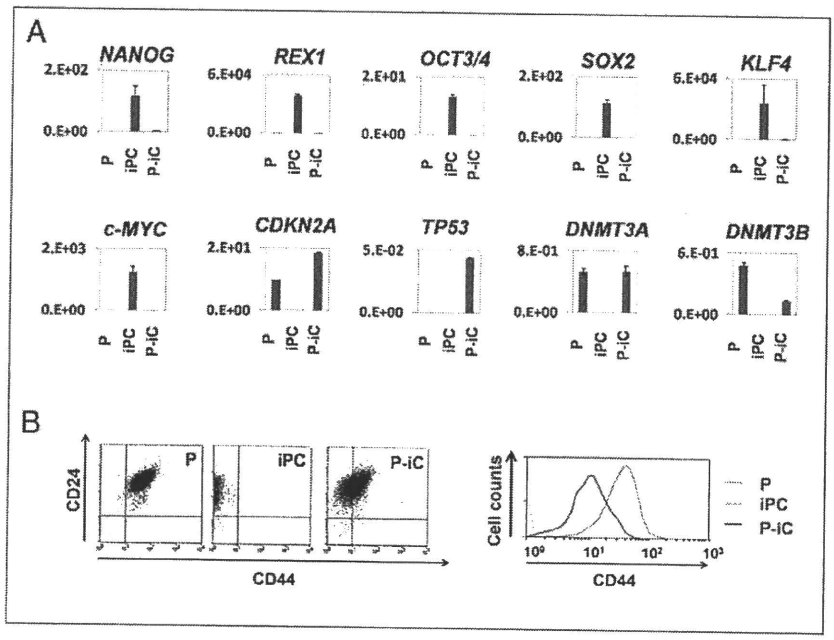

Fig. 5. Expression of immature and differentiated status-related genes in parental, iPC, and PostiPC cells induced from DLD-1. (*A*) The expression of *NANOG, REX1, OCT3/4, SOX2, KLF4, and c-MYC* markedly decreased in iPC cells. The expression of *CDKN2A, DNMT3A,* and *DNMT3B* increased in PostiPC cells compared to iPC cells. The mRNA copy expression was normalized against *GAPDH* mRNA expression. (*B*) (*Left*) Flow cytometry showed a shift of the CD24/CD44 population in parental, iPC, and PostiPC cells. (*Right*) The CD44 population in PostiPC cells decreased compared with that of parental cells. P, parental cells; P-iC, PostiPC cells.

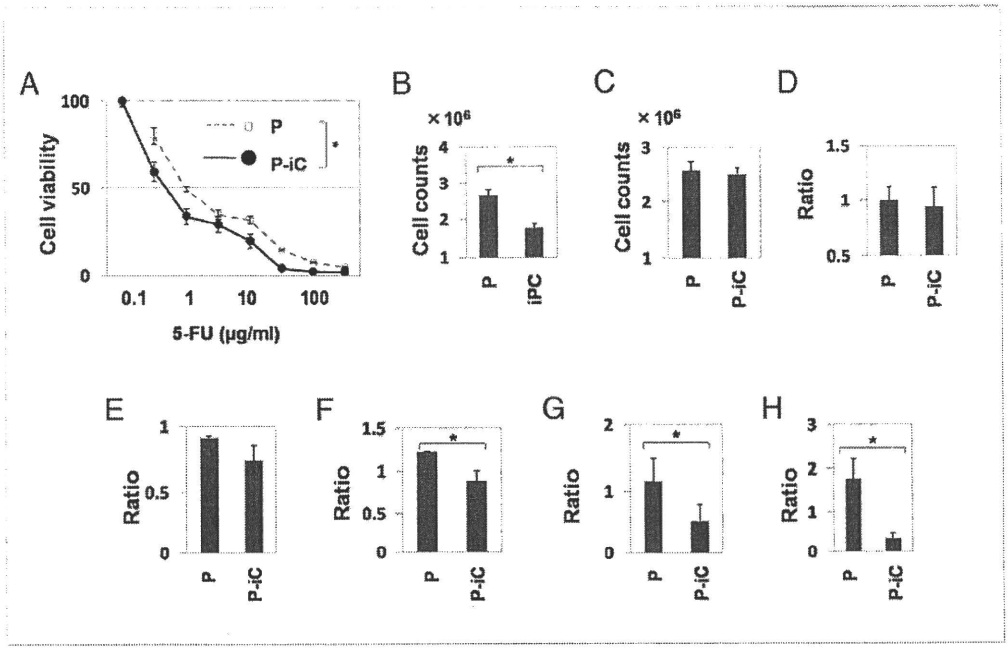

Fig. 6. In vitro methyl thiazolyl tetrazolium (MTT) analyses, proliferation and invasion assay. (*A*) The 5-FU MTT assay revealed significant differences in PostiPC and DLD-1 parental cells ($n = 11$, $P = 0.003$, Wilcoxon rank test). (*B*) Proliferation assays for ES-culture conditions showed differences in growth of iPC cells and DLD-1 parental cells ($n = 4$, $P = 0.046$, Wilcoxon rank test). (*C*) Proliferation assays in primary culture conditions showed no significant differences between DLD-1 parental and PostiPC cells. (*D*) Invasion assay showed no significant differences between DLD-1 parental and PostiPC cells (relative ratio and parental cell average). (*E* and *F*) Proliferation assays showed differences in ratio with control (with no treatment) under the differentiation-inducing treatment with vitamins A and D supplementation ($n = 8$, $P = 0.512$ and 0.049, respectively, Wilcoxon rank test). (*G* and *H*) Invasion assays showed significant differences in the ratio with control (with no treatment) cells under the differentiation-inducing treatment with vitamin A and D supplementation ($n = 6$, $P = 0.013$ and 0.003, respectively, Wilcoxon rank test). P, parental cells; P-iC, PostiPC cells. *, $P < 0.05$.

state in living cells based on the results of previous studies. We investigated *NANOG* expression in gastrointestinal cancer cell lines, corresponding to human iPS cells and teratocarcinoma NTERA-2, which had higher *NANOG* expression. The expression could not be detected in PostiPC cells with this system. A low efficiency, as shown in iPS (6–9, 13, 14), suggests a possibility that only a minority of tumor cell lines possesses specific potential to obtain the property of iPC, or more likely that multiple mechanisms are involved in full execution of reprogramming. We have to consider a possibility that sphere-forming cells might be rare among the original cancer cell populations.

In this study, the tumor-suppressor gene *P16(INK4A)*, which acts against the self-renewal of ES cells (10, 12), was repressed in iPC cells. Our analysis indicated that *P16(INK4A)* expression increased in PostiPC cells, which may relate to the notion that *P16(INK4A)* up-regulation is involved in the suppression of transformed phenotypes and their sensitization to therapeutic agents (24). The sequence study of *P16(INK4A)* promoter indicated the demethylation in PostiPC cells from DLD-1 cells, whereas the sequence of parental cells was methylated. This study suggests that the reactivation of tumor suppressor genes by reprogramming may play a role in increased chemosensitivity to 5-FU and the regression of cell proliferation and invasiveness under differentiation-inducing conditions. The *Rb/P16(INK4A)* tumor-suppressive pathway has been reported to be abrogated in several tumors (24). It is necessary to investigate the specific analysis in the pathways to assess the contribution of TSG.

Presumably, the suppression of tumors and their sensitization to induced differentiation are the result of genetic and epigenetic modifications. This result supports the possibility of new cancer therapies via reprogramming approaches even in cancer cells that should have corrupted genetic codes. In the present study, iPC cells were induced from eight cancer cells, including cancers of colorectum, esophagus, stomach, pancreas, liver and bile ducts (Fig. S4). Here, iPC was established from cancer cell lines. It is necessary to demonstrate universality in primary tumors and to more efficiently investigate the factors and population in relation to the induction of iPC cells: points to be elucidated and developed include differences of normal and tumor cells, individual responses, efficiency, and reagent delivery system. As novel therapeutic approaches, the heterogeneity of reprogrammed cancer cells remains to be investigated.

Materials and Methods

Cell Lines and Culture. Twenty cell lines derived from human gastrointestinal cancers included colorectal cancer (Caco2, DLD-1, HCT116, HT-29, KM12SM, LoVo, and SW480), esophageal cancer (TE-10), gastric cancer (MKN45), pancreatic cancer (BXPC-3, MIAPaCa-2, PANC-1, and PSN-1), hepatocellular carcinoma (Hep3B, HepG2, HLE, HLF, HuH-7, and PLC), cholangiocellular carcinoma (HuCCT-1), and teratocarcinoma (NTERA-2 clone D1). NTERA-2 was provided by DS Pharma Biomedical (Osaka). These cell lines were maintained in DMEM (Nakalai Tesque, Kyoto) containing 10% FBS at 37 °C under a 5% humidified CO_2 atmosphere. HDF was purchased from Toyobo (CA106K05a; Osaka) as a normal cell control and maintained with the Fibroblast Growth Medium kit (CA116500; Toyobo). Plasmids were purchased from Addgene (Cambridge, MA), Clontech (Palo Alto, CA), Cell Biolabs (San Diego), and Open Biosystems (Huntsville, AL). The plasmids used in this study are summarized in Table S1. These transfectants were grown in DMEM supplemented with 10% FBS and puromycin (2 μg/mL), and transferred to specific culture conditions as described in the supporting information. All transfectants with retrovirus were made with the ViraDuctin retrovirus transduction kit (Cell Biolabs). Those with lentivirus were made with the Virapower packaging mix (Invitrogen, Carlsbad, CA) or Arrest-In (Open Biosystems). In brief, cancer cell lines were transfected with adequate plasmid at a concentration of 4 μg/μl by using lipofectamine (Lipofectamine 2000; Invitrogen), and incubated in glucose-free Opti-MEM (Invitrogen). All experiments were performed at 50–70% cell confluence and results were confirmed in at least three independent experiments. All-in-one-type fluorescence microscopy

(BZ-8000; Keyence, Osaka) with digital photographic capability was used to visualize cells at several magnifications. The growth rates of the cultured gastrointestinal cancer cell lines were measured by counting cells using CellTac (Nihon Koden, Tokyo). The optimization of retroviral transduction of human cancer cell lines was performed as shown in supporting information. Vectors used are shown in Table S1.

RNA Preparation and RT-PCR. Total RNA was prepared by using TRIzol reagent (Invitrogen). Reverse transcription was performed with SuperScriptIII (Invitrogen). To confirm PCR amplification, 25–35 cycles of the PCR were performed by using a PCR kit (Takara, Kyoto) on a Geneamp PCR system 9600 (PE Applied Biosystems, Foster City, CA) with the following condition: 95 °C for 10 s, 60 °C for 10 s, and 72 °C for 60 s. An 8-μl aliquot of each reaction mixture was size-fractionated in a 1.5% agarose gel and visualized with ethidium bromide staining. To confirm RNA quality, PCR amplification was performed for the glyceraldehyde-3-phosphate dehydrogenase (*GAPDH*) gene using the specific primers (Tables S2 and S3). For quantitative assessment, we evaluated the gene expression by RT-PCR analysis. Quantitative real-time RT-PCR was performed by using a LightCycler TaqMan Master kit (Roche Diagnostics, Tokyo) for cDNA amplification of target specific genes. The expression of mRNA copies was normalized against *GAPDH* mRNA expression. The detailed condition for Quantitative real-time RT-PCR assessment is shown in supporting information. Primers used are shown in Tables S2 and S3.

Drugs and Antibodies. Antibodies used for immunocytology were against Nanog, Ssea-3, Ssea-4, Tra-1-60, Tra-1-81, Tra-2-49, Tubb3, Gfap, Vim (Chemicon International, Temecula, CA), and Krt19 (OriGene Technologies, Rockville, MD). Differentiation to adipocytes was induced by specific supplements (Adipogenic Supplement 390416; Invitrogen).

Bisulfite Sequencing. Genomic DNA was treated with Applied Biosystems methySEQr Bisulfite Conversion kit (Applied Biosystems) according to the manufacturer's recommendations. Treated DNA was purified with QIAquick column (Qiagen, Valencia, CA). The human *NANOG* gene promoter regions were amplified by PCR. The PCR products were subcloned with pCR2.1-TOPO. Every clone of each sample was verified by sequencing with the T3 and T7 primers. The analysis used Sequencing Analysis Software v5.2 (Applied Biosystems). Primer sequences used for PCR amplification are provided in Table S3.

Chromatin Immunoprecipitation Assay. Approximately 1×10^7 cells were cross-linked with 1% formaldehyde for 10 min at room temperature and quenched by adding glycine. The cell lysate was treated to share a chromatin-DNA complex with an enzymatic shearing kit (Active Motif, Carlsbad, CA). Immunoprecipitation used Protein G magnetic beads (Active Motif)-linked anti-trimethyl lysine 4 histone H3 antibody (Nippongene, Toyama, Japan), or a negative control IgG kit (Active Motif). Eluates were used as templates for quantitative PCR. Each sheared chromatin sample was used for quantitative PCR as a control. Primer sequences used for PCR amplification are provided in Table S3.

Flow Cytometry. Flow cytometry was performed on trypsin-dissociated parental cells, iPC, and PostiPC cells by using antibodies for CD24 (BD Biosciences, Sparks, MD) and CD44 (BD Biosciences). 7-AAD (eBioscience, San Diego, CA) preincubation was used to exclude dead cells. To assess the expression of the reprogrammed cells, iPC cells were assessed in the isolated colonies after the transfection of *NANOG* promoter-*GFP* clone. Cells were analyzed by using a FACScan flow cytometer equipped with CellQuest software (FACS caliber; BD Biosciences).

RA and VD3 Treatment. RA and VD3 were purchased from Sigma–Aldrich (St. Louis). RA was dissolved in 99% ethanol as a 100 μM stock solution. The cells were allowed to settle for 48 h in DMEM supplemented with 100 nM RA. VD3 was dissolved in 99% ethanol as a 10 M stock solution. The cells were allowed to settle for 48 h in DMEM supplemented with 10 nM VD3. To assess the proliferation in the presence of RA and VD3, the cells were grown in these media for another 48 h. Cell viability was determined with the Cell Counting kit incorporating WST-8 (Dojindo Lab., Tokyo). WST-8 (10 μL) was added to 100 μL of the medium containing each supplement above, and the absorbance was read at 450 nm by using a microplate reader (Model 680XR; Bio-Rad Laboratories, Hercules). All experiments were performed at 30–80% cell confluence, and the results were confirmed in at least three independent experiments.

Chemosensitivity Assessment. To assess the sensitivity to 5-FU in vitro, cells at different concentrations were evaluated with an MTT assay. 5-FU was purchased from Kyowa Hakkou (Tokyo). The cells were allowed to settle for 96 h in DMEM supplemented with several concentrations of 5-FU, and viability was assessed.

Invasion Assays. Cell invasion was assessed with a CytoSelect Cell Invasion Assay according to the manufacturer's protocol (Cell Biolabs). Cells (1.0×10^5) in DMEM were placed on 8.0-m-pore size membrane inserts in 96-well plates, and DMEM with 10% FBS was placed in the bottom of the wells. After 24 h, cells that did not invade were removed from the top side of the membrane chamber, and the cells from the underside of the membrane were completely dislodged by tilting the membrane chamber in Cell Detachment Solution (Cell Biolabs). Lysis Buffer/CyQuannt GR dye solution (Cell Biolabs) was added to each well, and the fluorescence of the mixture was read with a fluorescence plate reader at 480 nm/520 nm.

In Vivo Analysis. The tumorigenic properties were evaluated on trypsin-dissociated cells with parental and PostiPC cells. We transplanted them suspended in DMEM/Matrigel (BD Biosciences) s.c. into the dorsal flanks of NOD/SCID mice (CREA, Tokyo) in several concentrations. Tumors were dissected and measured 4 weeks after injection.

Statistical Analysis. For continuous variables, the results are expressed as means ± SEs of the mean. The relationships among gene expressions or cell counts were analyzed with χ^2 and Wilcoxon rank tests. All tests were analyzed with JMP software (SAS Institute, Cary, NC). Differences with P values <0.05 were considered statistically significant.

1. Reya T, Morrison SJ, Clarke MF, Weissman IL (2001) Stem cells, cancer, and cancer stem cells. *Nature* 414:105–111.
2. Pardal R, Clarke MF, Morrison SJ (2003) Applying the principles of stem-cell biology to cancer. *Nat Rev Cancer* 3:895–902.
3. Bonnet D, Dick JE (1997) Human acute myeloid leukemia is organized as a hierarchy that originates from a primitive hematopoietic cell. *Nat Med* 3:730–737.
4. Thomson JA, et al. (1998) Embryonic stem cell lines derived from human blastocysts. *Science* 282:1145–1147.
5. Hochedlinger K, Jaenisch R (2006) Nuclear reprogramming and pluripotency. *Nature* 441:1061–1067.
6. Takahashi K, Yamanaka S (2006) Induction of pluripotent stem cells from mouse embryonic and adult fibroblast cultures by defined factors. *Cell* 126:663–676.
7. Takahashi K, et al. (2007) Induction of pluripotent stem cells from adult human fibroblasts by defined factors. *Cell* 131:861–872.
8. Yu J, et al. (2007) Induced pluripotent stem cell lines derived from human somatic cells. *Science* 318:1917–1920.
9. Yu J, et al. (2009) Human induced pluripotent stem cells free of vector and transgene sequences. *Science* 324:797–801.
10. Dabelsteen S, et al. (2009) Epithelial cells derived from human embryonic stem cells display p16INK4A senescence, hypermotility, and differentiation properties shared by many P63+ somatic cell types. *Stem Cells* 27:1388–1399.
11. Hong H, et al. (2009) Suppression of induced pluripotent stem cell generation by the p53-p21 pathway. *Nature* 460:1132–1135.
12. Li H, et al. (2009) The Ink4/Arf locus is a barrier for iPS cell reprogramming. *Nature* 460:1136–1139.
13. Loh YH, et al. (2006) The Oct4 and Nanog transcription network regulates pluripotency in mouse embryonic stem cells. *Nat Genet* 38:431–440.
14. Wu Q, et al. (2006) Sall4 interacts with Nanog and co-occupies Nanog genomic sites in embryonic stem cells. *J Biol Chem* 281:24090–24094.
15. Adewumi O, et al.;International Stem Cell Initiative (2007) Characterization of human embryonic stem cell lines by the International Stem Cell Initiative. *Nat Biotechnol* 25: 803–816.
16. Vermeulen L, et al. (2008) Single-cell cloning of colon cancer stem cells reveals a multi-lineage differentiation capacity. *Proc Natl Acad Sci USA* 105:13427–13432.
17. Du L, et al. (2008) CD44 is of functional importance for colorectal cancer stem cells. *Clin Cancer Res* 14:6751–6760.
18. Huang ME, et al. (1988) Use of all-trans retinoic acid in the treatment of acute promyelocytic leukemia. *Blood* 72:567–572.
19. zur Nieden NI, Kempka G, Ahr HJ (2003) In vitro differentiation of embryonic stem cells into mineralized osteoblasts. *Differentiation* 71:18–27.
20. Singh SK, et al. (2004) Identification of human brain tumour initiating cells. *Nature* 432:396–401.
21. Kim CF, et al. (2005) Identification of bronchioalveolar stem cells in normal lung and lung cancer. *Cell* 121:823–835.
22. O'Brien CA, Pollett A, Gallinger S, Dick JE (2007) A human colon cancer cell capable of initiating tumour growth in immunodeficient mice. *Nature* 445:106–110.
23. Hahn WC, Weinberg RA (2002) Rules for making human tumor cells. *N Engl J Med* 347:1593–1603.
24. Sherr CJ, McCormick F (2002) The RB and p53 pathways in cancer. *Cancer Cell* 2: 103–112.

Clinical Cancer Research

Overexpression of miR-200c induces chemoresistance in esophageal cancers mediated through activation of the Akt signaling pathway

Rie Hamano, Hiroshi Miyata, Makoto Yamasaki, et al.

Clin Cancer Res Published OnlineFirst January 19, 2011.

Author Manuscript Published OnlineFirst on January 19, 2011; DOI:10.1158/1078-0432.CCR-10-2532
Author manuscripts have been peer reviewed and accepted for publication but have not yet been edited.

Overexpression of miR-200c induces chemoresistance in esophageal cancers mediated through activation of the AKT signaling pathway

Rie Hamano, Hiroshi Miyata, Makoto Yamasaki, Yukinori Kurokawa, Johji Hara, Jeong ho Moon, Kiyokazu Nakajima, Syuji Takiguchi, Yoshiyuki Fujiwara, Masaki Mori and Yuichiro Doki

Department of Gastroenterological Surgery, Osaka University Graduate School of Medicine, Suita, Yamadaoka 2-2, Osaka 565-0871, Japan

Running title: Chemoresistance in esophageal cancer and miR-200c expression

Address for correspondence and reprint requests:

Hiroshi Miyata, MD, PhD,
Department of Gastroenterological Surgery,
Osaka University Graduate School of Medicine,
2-2, Yamadaoka, Suita,
Osaka 565-0871, Japan
Tel: +81-6-6879-3251
Fax: +81-6-6879-3259
E-mail: hmiyata@gesurg.med.osaka-u.ac.jp

Abstract

Purpose To determine the relationship between resistance to chemotherapy and microRNAs (miRNAs) expression in esophageal cancer, we focused on miRNAs known to be related to maintenance of stem cell function.

Experimental Design Using 98 formalin-fixed paraffin-embedded samples from patients with esophageal cancer who had received preoperative chemotherapy followed by surgery, we measured the expression levels of several miRNAs that are considered to be involved in the regulation of stem cell function (let-7a, let-7g, miR-21, miR-134, miR-145, miR-155, miR-200c, miR-203 and miR-296) by real-time reverse transcription-PCR. The, we examined the relationship between miRNA expression and prognosis or response to chemotherapy. To investigate the mechanism of miRNA-induced chemoresistance, *in vitro* assays were performed using esophageal cancer cells.

Results Analyses of the nine miRNAs expression showed that overexpression of miR-200c (P=0.037), underexpression of miR-145 (P=0.023) and overexpression of miR-21 (P=0.048) correlated significantly with shortened overall survival. In particular, miR-200c expression correlated significantly with response to chemotherapy (P=0.009 for clinical response, P=0.007 for pathological response). *In vitro* assay showed significantly increased miR-200c expression in cisplatin-resistant cells compared with their parent cells (~1.7-fold). In anti-miR-200c transfected cells, chemosensitivity to cisplatin and apoptosis after exposure to cisplatin increased compared with the negative control. Western blotting showed that knockdown of miR-200c expression was associated with increased expression of PPP2R1B, a

subunit of protein phosphatase 2A, which resulted in reduced expression of phospho-Akt.

Conclusions Our results emphasized the involvement of miR-200c in resistance to chemotherapy in esophageal cancers and that this effect was mediated through the Akt pathway.

Key words microRNA, esophageal cancer, resistance, chemotherapy, prognosis

Translational Relevance

In this study, we examined the expression of several miRNAs known to regulate stem cell function in formalin-fixed paraffin-embedded tissues from patients with esophageal cancer who received preoperative chemotherapy followed by surgery. The results showed that overexpression of miR-200c was closely associated with poor response to preoperative chemotherapy and poor prognosis, and in the in vitro study, we found that miR-200c directly targeted PPP2R1B, and resulted in activation of Akt signaling. The results suggested that miR-200c is a potentially useful predictor of chemosensitivity in patients with esophageal cancer.

Introduction

Esophageal cancer is the eighth most common incident cancer and sixth most common cause of cancer death (1). Surgery is regarded as standard management for esophageal cancer, but the prognosis of patients who receive only surgery is poor with a 5-year survival rate ranging from 15% to 39% (2,3). To improve survival of patients with esophageal cancer, multimodal treatment, including chemotherapy plus surgery and chemoradiotherapy plus surgery have been developed. In fact, some clinical trials showed that these multimodal therapies prolonged survival of esophageal cancer patients (4,5). The most commonly used chemotherapeutic regimen in esophageal cancers is cisplatin-based chemotherapy, such as combination chemotherapy of cisplatin and 5-fluorouracil (5-FU). However, the reported response rate to chemotherapy including cisplatin is only 19-40% (3,6), and about half of the patients do not achieve good response to chemotherapy. Thus, chemoresistance is a major obstacle in the treatment of esophageal cancers. A better understanding of the mechanism of chemoresistance in esophageal cancer is needed to improve prognosis.

MicroRNAs (miRNAs) bind to the 3' untranslated region of their target mRNAs and such binding leads to translational repression or reduced stability of the mRNA (7). MiRNAs play important roles in various biological processes, such as cell differentiation, cell proliferation, apoptosis, and metabolism. In addition, miRNAs have emerged as central regulators of cancer (8), and their aberrant expression in many tumors indicate that they could function as tumor suppressors or oncogenes.

Recent studies showed that some miRNAs (e.g., let-7, miR-134, miR-296, miR-302, miR-367, and miR-470) are involved in the regulation of stem cell function such as self-renewal, pluripotency and differentiation (9,10). MiR-145 directly regulates the reprogramming factors (OCT4, SOX2 and KLF4) and inhibits human ES cell self-renewal, represses the expression of pluripotency genes (11), while miR-203 directly represses the expression of p63, which is an essential regulator of stem cell maintenance in epithelial tissues (12). On the other hand, the "cancer stem cells (CSCs)" hypothesis has attracted lots of attention. This hypothesis suggests that cancers are maintained in a hierarchical organization of rare, slowly dividing cancer stem cells (or tumor-initiating cells), rapidly dividing amplifying cells and differentiated tumor cells. There are several similarities between CSCs and normal stem cells with respect to maintaining self-renewal and pluripotency. Therefore, miRNA may play an important role in the regulation of CSCs as well as normal stem cells. In fact, a recent study showed accumulation of tumor initiating cells after initiation of chemotherapy in breast cancer and reduced let-7 expression in these tumor initiating cells, which helped maintain the undifferentiated status and proliferative potential (13). CSCs cells are considered responsible for resistance to anticancer treatment such as chemotherapy and radiotherapy (14).

The main hypothesis of the present study was that miRNAs that regulate stem cell function are involved in resistance to chemotherapy in esophageal cancer. To test the hypothesis, we examined the expression levels of several miRNAs considered to be involved in the maintenance of stem cell function, such as let-7 family, miR-145, miR-200c, miR-21, miR-296, miR-155 miR-134 and miR-296, and analyzed their